Available online at www.sciencedirect.com
ScienceDirect
Journal of Magnetic Resonance 190 (2008) 149–153
JMR Journal of Magnetic Resonance
www.elsevier.com/locate/jmr

Communication

Enhancement of magnetization transfer effects by inter-molecular multiple quantum filtered NMR

Uzi Eliav, Gil Navon *

School of Chemistry, Tel Aviv University, Ramat Aviv, Tel Aviv 69978, Israel

Received 10 May 2007
Available online 23 October 2007

Abstract

There are a number of methods that give MRI contrasts based on changes of the water M_z magnetization as a result of magnetization transfer to macromolecules. In the present work we report that a combination of these methods with inter-molecular multiple quantum coherences (iMQC) gives enhanced effects. For the magnetization transfer contrast (MTC) method an effect of (M_z/M_0) becomes $(M_z/M_0)^l$ where l is the rank of the tensors constituting the iMQC. A similar trend was found upon combining iMQC with the Goldman–Shen experiment. It is pointed out that the method is general for all magnetization transfer methods, including the nuclear Overhauser effect.

Keywords: iMQC; Intermolecular dipolar interaction; Magnetization transfer; MTC; Goldman–Shen

1. Introduction

Inter-molecular multiple quantum coherences resulting from correlations between spins residing on separate molecules in liquids were demonstrated in many systems, in vitro and in vivo yielding a new kind of MRI contrast sensitive to the proton density and structural properties of the sample. (iMQC experiments) [1–7]. The sensitivity to the type and the amounts of the macromolecules in the sample is similar to that obtained in the standard, single-quantum, MRI experiments where the contrasts are based on intra-molecular dipolar interactions. Sensitivity to the macromolecular content of the tissue has been obtained by a variety of methods such as magnetization transfer contrast (MTC) [8], Goldman–Shen (GS) [9,10], Edzes–Samulski (ES) [11] double quantum filtered-magnetization transfer (DQF-MT) [12] and magnetization exchange imaging (MEXI) [13]. Here we report that combinations of iMQC with MTC and with GS give a very significant increase in the contrast over those achieved by these two methods alone.

* Corresponding author.
E-mail address: navon@post.tau.ac.il (G. Navon).

1090-7807/$ - see front matter © 2007 Elsevier Inc. All rights reserved.
doi:10.1016/j.jmr.2007.09.017

2. Materials and methods

Experiments were performed on two types of samples: (a) excised bovine optic nerve (b) 10% w/w Bovine serum albumin (BSA) dissolved in 80% D_20 and 20% water and the same solution of BSA that was crosslinked by treatment with 50 μl/ml of 25% solution of glutaraldehyde [14,15]. The sample in (b) consisted of two concentric tubes, of 10 mm containing the untreated BSA and of 5 mm containing the treated material. All experiments on samples of type (a) were conducted on a Bruker AVANCE 11.74 T spectrometer with either 5 or 10 mm probes detuned by at least 4 MHz (i.e. offset $\geqslant 4\omega_o/Q$). The detuning and the usage of deuterated solvent were done in order to reduce radiation damping effects. The BSA samples (type (b)) were measured on Bruker Avance WB 8.45 T spectrometer equipped with micro-imaging accessory.

2.1. Pulse sequences

Pulse sequences that combine iMQC [1–7] with variety of methods that facilitate the measurement of magnetization transfer are presented. The methods to be combined are MTC [8], Goldman–Shen [9,10] and the Edzes–Samulski [11].

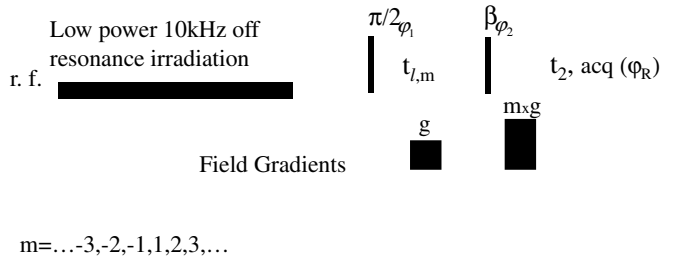

Fig. 1. The pulse sequence that combines MTC with iMQC.

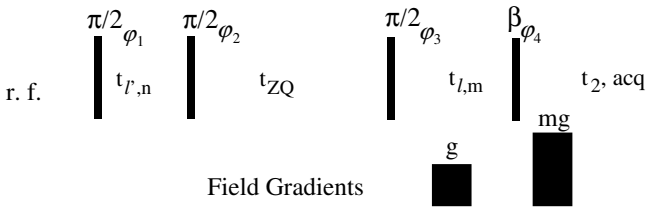

Fig. 3. A schematic presentation of pulse sequences that combine iMQC with GS-like experiments.

Fig. 1 describes the iMQC pulse sequence [1–3] that is modified to include the MTC effect [8] by inserting a low power off resonance cw irradiation prior to the first pulse.

The iMQC pulse sequence is based on the presence at equilibrium of the high rank tensors $\prod_{i=1}^{l} I_{zi}$ where l is the rank of the selected coherence during the period t_{lm} and I_{zi} are the z component of the spins of protons residing on distant solvent molecules. The coherence selection is accomplished by the application of two gradients with intensity ratio m together with a suitable phase cycling that prevents the effects of field inhomogeneities.

If we assume that during the pre-saturation period the longitudinal magnetization of the water protons reach a steady state that is affected predominantly by interactions with macromolecules, the signal of the iMQC experiment will be proportional to $\prod_{i=1}^{l} I_{zi}(\textit{steady state})$. For instance if $m = 2$ the signal would be proportional to $I_{z1}(\textit{steady state})I_{z2}(\textit{steady state})$. If we further assume that the MTC effect is similar all over the sample the reduction of the water signal upon off-resonance irradiation, defined as $\eta = \text{Signal(saturate)/Signal(unsaturated)}$, will be $\eta = (M_z/M_0)^2$ for the iDQC case, or $\eta = (M_z/M_0)^l$ for the general case of iMQC.

The above combination of iMQC with MTC can be implemented as a weighting step for imaging sequences (see Fig. 2) where β is selected as to maximize the transfer function of the spherical tensor $T_{l,m}$ to $T_{l,-1}$. For instance for iDQC $m = -2$ and $\beta = 60°$ (or 120° for $m = 2$). A zero quantum filter is added to reduce distortions due to evolution during the imaging period.

Enhanced contrast by combination with iDQC is not limited to MTC but should be obtained with any experiment which is based on modulation of the water I_z magnetization. Thus one can combine iDQC (or higher coherences) with Goldman–Shen (GS, 9) and similar experiments to augment their effects. A general scheme of such pulse sequence is shown in Fig. 3. For instance to combine the GS experiment with iDQC one selects $n = \pm 1$, $m = -2$ and $\beta = 60°$. Within that scheme it is also possible to describe the standard GS experiment choosing $n = \pm 1$, $m = 1$ and $\beta = 180°$.

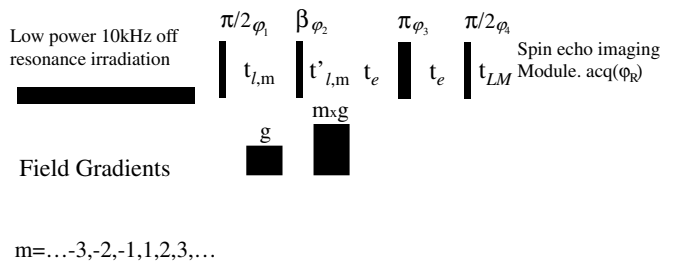

Fig. 2. The pulse sequence used for imaging the BSA samples. It was used either for conventional MTC i.e. $m = 1$ and $\beta = 180°$ or for the iDQC combined with MTC i.e $m = -2$ and $\beta = 60°$.

3. Results

3.1. Combining MTC with iMQC

A comparison between the conventional MTC experiment ($m = 1$ and $\beta = 180°$ in Fig. 1) and its combination with iDQC, applied to a sample of excised bovine optic nerve is given in Fig. 4. While the value of 0.38 was obtained for the MTC experiments the MTC-iDQC combination gives $\eta = 0.15$ (see Fig. 4). These results fit the theoretical prediction of $\eta = (M_z/M_0)^2$. Similar trends were obtained for the BSA samples where we confirmed the $(M_z/M_0)^2$ dependence on the saturation level.

3.2. Imaging using the iDQC combined with MTC

In Fig. 5 we demonstrate the effect of pre-saturation on the contrast between a BSA solution that was treated with glutaraldehyde and the one that was not treated. For the untreated BSA solution in the outer tube no direct or indirect saturation effects were observed using the MTC sequence. Thus subtraction of the images of the untreated BSA obtained with and without pre-saturation (Fig. 5a and b, outer tube) yields a signal below the noise level. In the MTC-iDQC experiment some effect of the off-resonance irradiation could be detected but was too small to be quantitated.

On the other hand for the treated sample, in the inner tube, a very significant effect of the off-resonance irradiation was observed in both the MTC and the MTC-iDQC experiments (Fig. 5b and e). The difference between the two methods is demonstrated by the different values of η (Section 3.1). While for conventional MTC a value of $\eta = 0.53 \pm 0.025$ was observed, the MTC-iDQC experiment yielded a value of $\eta = 0.29 \pm 0.03$. Again, like in

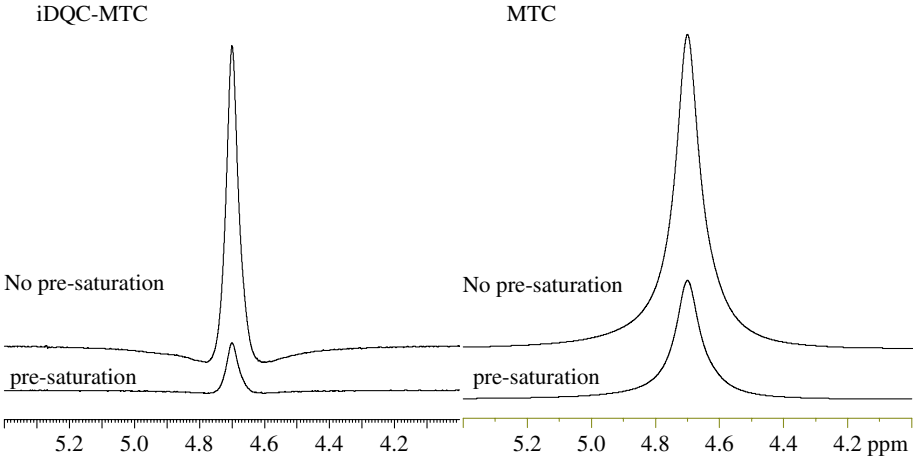

Fig. 4. MTC results for a sample of excised bovine optic nerve. Left hand side presents the results of MTC combined with iDQC (Fig. 1 with $m = -2$ and $\beta = 60°$); the right hand side shows the conventional MTC. The strength of the r.f. magnetic field of the 10 kHz off-resonance irradiation was 2.8 μT and its duration 1 s.Gradient strength (g in Fig. 1) was 18.4 G/cm and its duration 0.5 ms. The phase cycling used to obtain the results of the iDQC combined with MTC experiment was: $\varphi_1 = k \times 45°$, $\varphi_2 = l \times 90°$, $\varphi_R = k \times 90° + l \times 270°$ with $k = 0, 1, 2, 3, 4, 5, 6, 7$ and $l = 0, 1, 2, 3$.

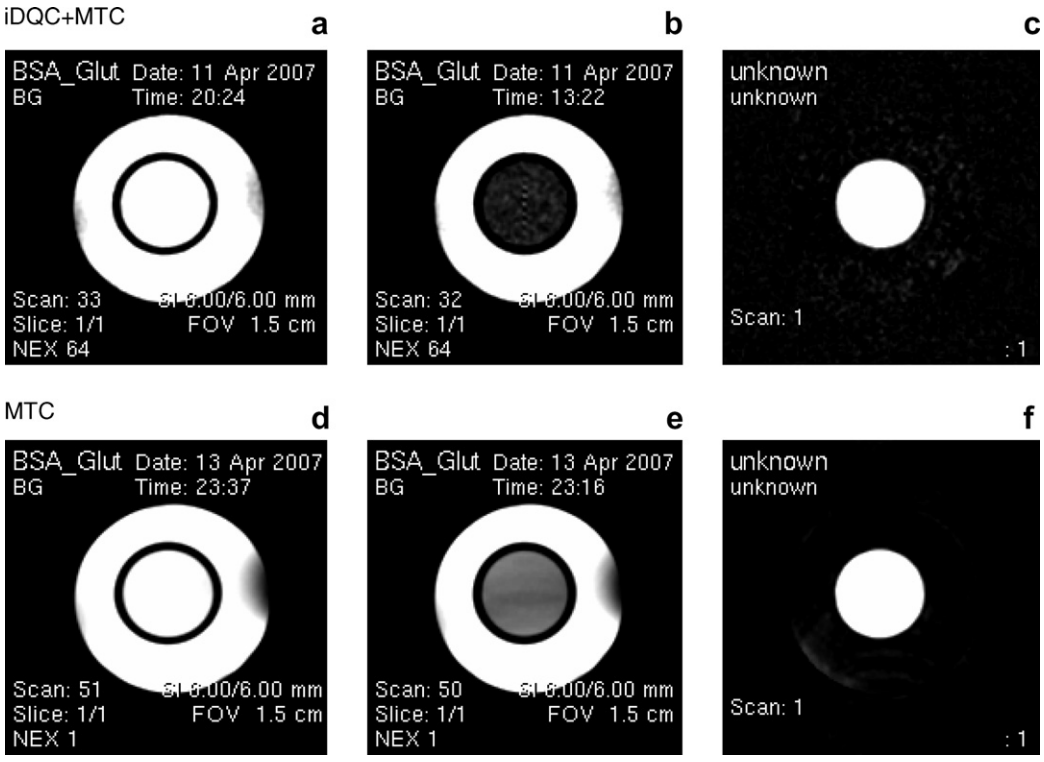

Fig. 5. Images of a phantom containing solutions of BSA (outer tube) and of cross-linked BSA (inner tube). The images were acquired by the pulse sequence given in Fig. 2, with either $m = -2$ and $\beta = 60°$ (Fig. 5a–c) (MTC+iDQC) or $m = 1$ and $\beta = 180°$ (Fig. 5d–f) (MTC). The strength of the 10 kHz off-resonance cw irradiation was 2 μT and its duration 1 s.Gradient strength (g in Fig. 2) was 73.6 G/cm and its duration 0.4 ms. Other intervals values are: $t_{lm} = 50$ μs. $t'_{lm} = 550$ μs, $t_e = 35$ ms, TE = 12.4 ms, TR = 5 s. The imaging pulse sequence was a standard fast spin echo with two echoes in each scan and a matrix size of 128×128. All echoes times (t_e and T_E) were kept shorter than T_2 so that T_2 weighting will not affect significantly the contrast (Fig. 5a and d). For the MTC experiments the number of accumulations was 1 while for its combination with iDQC it was 64 with the following phase cycling: $\varphi_1 = k_1 \times 45°$, $\varphi_2 = k_2 \times 90°$, $\varphi_3 = k_4 \times 180°$, $\varphi_4 = \varphi_3$, $\varphi_R = k_1 \times 90° + k_2 \times 270° + k_4 \times 180°$ with $k_1 = 0, 1, 2, 3, 4, 5, 6, 7$, $k_2 = 0, 1, 2, 3$ and $k_4 = 0, 1$.

the spectroscopic experiments the MTC and the MTC-iDQC gave effects corresponding to (M_z/M_0) and $(M_z/M_0)^2$, respectively. One should note that while the contrast to noise ratio (CNR) between the two compartments obtained with the iDQC-MTC (Fig. 5b) is half that obtained with conventional MTC (Fig. 5e) the CNR per scan obtained with the iDQC-MTC is inferior by a factor of 16.

3.3. Combining GS with iMQC

In the standard GS [9] $n = \pm 1$, $m = 1$, $\beta = 180°$ (Fig. 3) and the $t_{l',n}$ period is selected so that the macromolecules are decaying off while the water magnetization is hardly affected. Thus the signal dependence on the t_{ZQ} period, assuming two pools under fast exchange condition, is given by [10,11]:

$$S(I_z^1) \sim 1 + P_p(e^{-kt_{ZQ}} - e^{-t_{ZQ}/T_1}) \quad (1)$$

where k is the sum of the rates of the forward and backward exchange reactions, T_1 is the longitudinal relaxation time and P_p is the fraction of the macromolecule. For bovine optic nerve the signal dependence on t_{ZQ} is given by the upper trace in Fig. 6. A fast decay due to the chemical exchange is evident on the time scale of tens of ms ($k = 20\ s^{-1}$). The slower recovery time, 1.8 s, is identical to the value obtained for T_1 in inversion recovery experiment.

Upon combining the GS with iDQC (selecting $n = 1$, 2 and $m = -2$ in the sequence shown in Fig. 3) the resulting tensors are better described by spherical tensors $T_{l,\ m}$ that contain also the flip–flop terms $I_{+1}I_{-2}$. At very short t_{ZQ} these tensors are: $T_{1,0}$ and $T_{2,0}$ and their proportion is the same as at equilibrium i.e. before the first pulse in Fig. 3. Under these conditions, and under the assumption that the contributions of inter-molecular dipolar interactions to the longitudinal relaxation can be neglected, the only important dynamic is magnetization transfer with the protein and thus the evolution of the signal that follows the dynamic of the tensor $I_{z1}I_{z2}$, during t_{ZQ} is given by:

$$S(I_z^1 I_z^2) \sim (1 + P_p(e^{-kt_{ZQ}} - e^{-t_{ZQ}/T_1}))^2 \quad (2)$$

The result in Eq. (2) resembles the one $S(I_{z1}I_{z2}) \sim (1 - e^{-t_{ZQ}/T_1})^2$ obtained by Chen et al. [16] who studied the combination of saturation recovery with iMQC. For bovine optic nerve the signal dependence on t_{ZQ} of the combination of GS with iDQC is given by the lower trace in Fig. 6. A fast decay due to the chemical exchange is evident on the time scale of tens of ms and the rate obtained for this process by fitting the data in Fig. 6 to the expression in Eq. (2) is identical with the one obtained from the conventional GS experiment ($20\ s^{-1}$). It is followed by the recovery to equilibrium due to the longitudinal relaxation. Clearly, as is predicted by Eq. (2), the minimum in the iDQC version is smaller than in the conventional MTC (upper trace in Fig. 6) experiment.

4. Discussion

In the present work the amplification of the contrast by combination with iMQC was demonstrated for the MTC and GS methods. Although the CNR per scan in this combination is inferior to that of the conventional methods it should be useful for cases where the noise level is not a limiting factor.

The effect of combining iDQC with magnetization transfer methods goes far beyond the two methods considered in

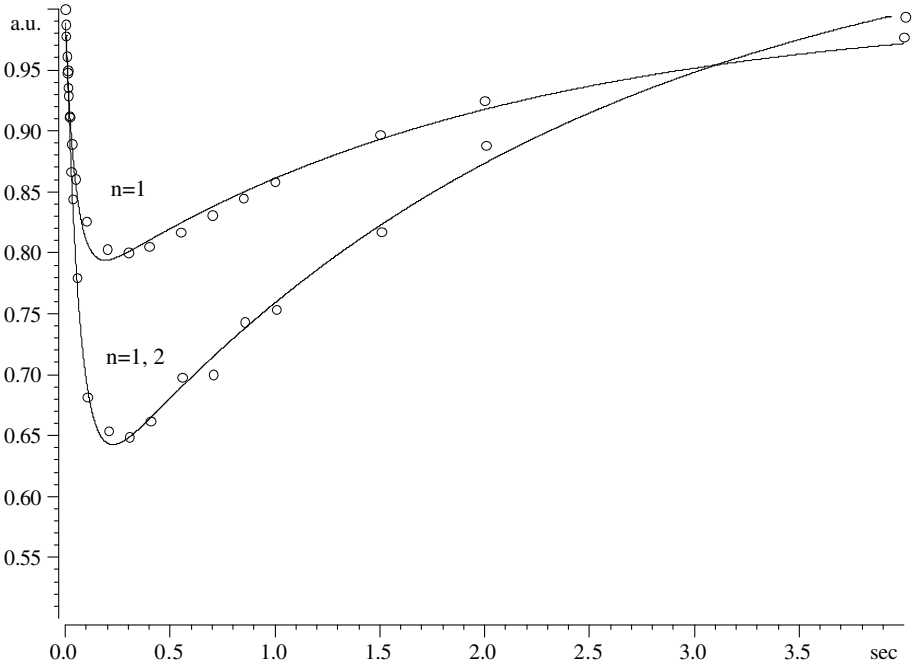

Fig. 6. The effect of iDQC on the Goldman–Shen experiment for an excised bovine optic nerve. The sequence is that given in Fig. 3 with $m = 1$ $n = \pm 1$ and $\beta = 180°$ for the upper trace (conventional GS sequence) and $m = -2$, $n = \pm 1$, ± 2 for the lower trace (GS + iDQC). $t_{l',n} = 100$ μs, $t_{l,m} = 50$ μs. Gradient strength was 73.6 G/cm and its duration 0.4 ms. The phase cycling used (a) lowest trace: $\varphi_1 = k_1 \times 180°$, $\varphi_2 = \varphi_1 + 180°$, $\varphi_3 = k_3 \times 45°$, $\varphi_4 = k_4 \times 180°$, $\varphi_R = k_3 \times 90° + k_4 \times 180°$ with $k_1 = 0$, 1, $k_2 = 0$, 1, $k_3 = 0$, 1, 2, 3, 4, 5, 6, 7, and $k_4 = 0$, 1. (b) Upper trace $\varphi_1 = \varphi_2 + 180° = k_1 \times 180°$, $\varphi_3 = k_3 \times 90°$, $\varphi_4 = k_4 \times 180°$, $\varphi_R = k_3 \times 270°$ with $k_1 = 0$, 1, $k_3 = 0$, 1, 2, 3, $k_4 = 0$, 1.

the current publication. It is general for all techniques that are based on changes in the longitudinal magnetization M_z. These include all those mentioned in the Introduction, namely ES, DQF-MT and MEXI, but also the methods designed to measure chemical exchange or getting contrast by saturation transfer such as the chemical exchange dependent saturation transfer (CEST) [17], paramagnetic CEST, (PARACEST) [18,19], as well as the many techniques based on the nuclear Overhauser effect (NOE).

Acknowledgment

This work was supported by a grant from the Israel Science Foundation.

References

[1] Q. He, W. Richter, S. Vathyam, W.S. Warren, Intermolecular multiple-quantum coherences and cross correlations in solution nuclear magnetic resonance, J. Chem. Phys. 98 (1993) 6779–6800.
[2] S. Lee, W. Richter, S. Vathyam, W.S. Warren, Quantum treatment of the effects of dipole–dipole interactions in liquid nuclear magnetic resonance, J. Chem. Phys. 105 (1996) 874–900.
[3] W.S. Warren, W. Richter, A.H. Addreotti, B.T. Farmer, Generation of impossible cross-peaks between bulk water and biomolecules in solution NMR, Science 262 (1993) 2005–2009.
[4] P.R. Bachiller, S. Ahn, W.S. Warren, Detection of intermolecular heteronuclear multiple-quantum coherences in solution NMR, J. Magn. Reson. A 122 (1996) 94–99.
[5] L.S. Bouchard, R.R. Rizi, W.S. Warren, Magnetization structure contrast based on intermolecular multiple-quantum coherences, Magn. Reson. Med. 48 (2002) 973–979.
[6] C.L. Chin, X.P. Tang, L.S. Bouchard, P.K. Saha, W.S. Warren, Isolating quantum coherences in structural imaging using intermolecular double-quantum coherence MRI, J. Magn. Reson 165 (2003) 309–314.
[7] L.S. Bouchard, F.W. Wehrli, C.L. Chin, W.S. Warren, Structural anisotropy and internal magnetic fields in trabecular bone: Coupling solution and solid dipolar interactions, J. Magn. Reson 176 (2005) 27–36.
[8] S.D. Wolff, R.S. Balaban, Magnetization transfer contrast (MTC) and tissue water proton relaxation in-vivo, Magnetic Resonance in Medicine 10 (1989) 135–144.
[9] M. Goldman, L. Shen, Spin–Spin Relaxation in Laf3, Physical Review 144 (1966) 321–331.
[10] J.P. Renou, M. Bonnet, G. Bielicki, A. Rochdi, P. Gatellier, NMR study of collagen–water interactions, Biopolymers 34 (1994) 1615–1626.
[11] H.T. Edzes, E.T. Samulski, Cross relaxation and spin diffusion in proton NMR of hydrated collagen, Nature 265 (1977) 521–523.
[12] A. Neufeld, U. Eliav, G. Navon, New MRI method with contrast based on the macromolecular characteri stics of tissues, Magn. Reson. Med. 50 (2003) 229–234.
[13] D. Carasso, U. Eliav, G. Navon, Nuclear magnetic resonance parameters for monitoring coagulation of liver tissue, Magn. Reson. Med. 54 (2005) 1082–1086.
[14] R.G. Bryant, D.A. Mendelson, C.C. Lester, The magnetic field dependence of proton spin relaxation in tissues, Magn. Reson. Med. 21 (1991) 117–126.
[15] S.H. Koenig, R.D. Brown III, R. Ugolini, Magnetization transfer in cross-linked bovine serum albumin solution at 200 MHz: a model for tissue, Magn. Reson. Med. 29 (1993) 311.
[16] Z. Chen, Z. Chen, J. Zhong, Quantitative study of longitudinal relaxation related to intermolecular dipolar interactions in solution NMR, Chem. Phys. Lett. 333 (2001) 126–132.
[17] K.M. Ward, A.H. Aletras, R.S. Balaban, A new class of contrast agents for MRI based on proton chemical exchange dependent saturation transfer (CEST), J. Magn. Reson 143 (2000) 79–87.
[18] M. Woods, D.E. Woessner, A.D. Sherry, Paramagnetic lanthanide complexes as PARACEST agents for medical imaging, Chem. Soc. Rev. 35 (2006) 500–511.
[19] S. Aime, C. Carrera, D. Delli Castelli, S. Geninatti Crich, E. Terreno, Tunable imaging of cells labeled with MRI-PARACEST agents, Angew. Chem. Int. Ed. Engl. 44 (2005) 1813–1815.